Provided for non-commercial research and education use.
Not for reproduction, distribution or commercial use.

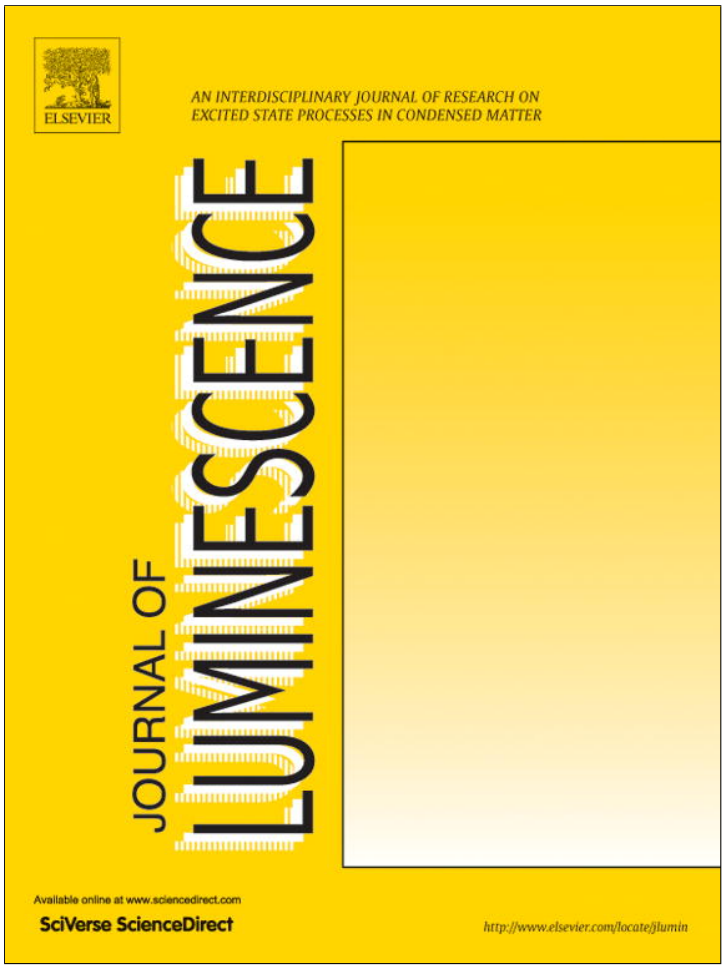

(This is a sample cover image for this issue. The actual cover is not yet available at this time.)

This article appeared in a journal published by Elsevier. The attached copy is furnished to the author for internal non-commercial research and education use, including for instruction at the authors institution and sharing with colleagues.

Other uses, including reproduction and distribution, or selling or licensing copies, or posting to personal, institutional or third party websites are prohibited.

In most cases authors are permitted to post their version of the article (e.g. in Word or Tex form) to their personal website or institutional repository. Authors requiring further information regarding Elsevier's archiving and manuscript policies are encouraged to visit:

http://www.elsevier.com/copyright

Author's personal copy

Journal of Luminescence 136 (2013) 270–277

Contents lists available at SciVerse ScienceDirect

Journal of Luminescence

journal homepage: www.elsevier.com/locate/jlumin

Thermal dependence of time-resolved blue light stimulated luminescence in α-Al_2O_3:C

Vasilis Pagonis [a,*], Christina Ankjærgaard [b], Mayank Jain [c], Reuven Chen [d]

[a] McDaniel College, Physics Department, Westminster, MD 21157, USA
[b] Netherlands Centre for Luminescence Dating, Technical University of Delft, The Netherlands
[c] Radiation Research Division, Risø National Laboratory for Sustainable Energy, Technical University of Denmark, DK-4000 Roskilde, Denmark
[d] Raymond and Beverly Sackler School of Physics and Astronomy, Tel Aviv University, Tel Aviv 69978, Israel

ARTICLE INFO

Article history:
Received 22 September 2012
Received in revised form
14 November 2012
Accepted 26 November 2012
Available online 3 December 2012

Keywords:
Time resolved photoluminescence
Photoluminescence
Pulsed luminescence
Al_2O_3:C
Luminescence lifetimes
Thermal quenching

ABSTRACT

This paper presents time-resolved optically stimulated luminescence (TR-OSL) experiments in the important dosimetric material Al_2O_3:C. During these experiments short pulses (0.5 s) of light from blue LEDs (470 nm) are followed by relaxation periods (2.5 s) of the charge carriers at different stimulation temperatures. During the pulse excitation period the integrated TR-OSL signal increases with the stimulation temperature between 50 and 150 °C, while between 160 and 240 °C the signal intensity decreases. This behavior is interpreted to arise from competing effects of thermal assistance (activation energy, $E_{th}=0.067\pm0.002$ eV) and thermal quenching (activation energy $W=(1.032\pm0.005)$ eV). Changes in the shape of the TR-OSL curves were analyzed at different stimulation temperatures using analytical expressions available in the literature. The TR-OSL signals contain a slower temperature-dependent phosphorescence signal, the "delayed-OSL" described previously for this material. The temperature dependent luminescence lifetimes obtained from analysis of the optical stimulation period are identical to those obtained from the corresponding relaxation period. However, the values of these luminescence lifetimes are systematically higher than previously reported values from time-resolved photoluminescence (TR-PL) studies carried out in this important dosimetric material. These results are discussed within the context of a recently published kinetic model.

© 2012 Elsevier B.V. All rights reserved.

1. Introduction

Luminescence lifetimes of insulators and semiconductors can be measured using time-resolved optically stimulated luminescence (TR-OSL) measurements, by experimentally separating the stimulation and emission of luminescence. This technique allows direct measurements of luminescence lifetimes and thus provides a means to investigate the luminescence pathways, and to estimate the delay between stimulation and emission of luminescence. Furthermore, this type of experiment can yield valuable information concerning the underlying luminescence mechanisms. For reviews of experimental and modeling studies involving time-resolved luminescence in a variety of natural and synthetic material, the reader is referred to the luminescence books by Bøtter-Jensen et al. [1], Yukihara and McKeever [2], and Chen and Pagonis [3].

TR-OSL measurements have been carried out rather extensively in quartz samples, due to the importance of this material in dating and retrospective dosimetry ([4–7] and references therein). Additionally, this technique has been applied in the study of feldspars ([8–13] and references therein), and as a dosimetry tool for Al_2O_3:C [2]. The dosimetric material Al_2O_3:C has been the subject of numerous experimental and modeling studies, due to its importance in radiation dosimetry ([14–26]). In most dosimetric applications with Al_2O_3:C, green light stimulation is used for OSL measurements, since green light provides efficient separation between the stimulation wavelength and the main luminescence band at ~420 nm [2].

Several studies have also used pulsing with blue light (~470 nm) using LEDs. Bulur et al. [27] reported that blue light causes phototransfer effects in α-Al_2O_3:C, while several additional studies showed that stimulation with short wavelengths can transfer charge carriers from deep traps into the main dosimetric traps [28–30]. Polymeris et al. [30] studied alumina using blue LEDs at 470 nm, and reported a thermally assisted OSL signal (TA-OSL) measured at elevated temperatures of 190 °C. Umisedo et al. [31] investigated the possibility of using blue light for optical stimulation in Al_2O_3:C, and examined whether this alternative wavelength of optical stimulation introduces problems not usually observed with green stimulation. Specifically these authors studied

* Corresponding author. Tel.: +1 410 857 2481; fax: +1 410 386 4624.
E-mail address: vpagonis@mcdaniel.edu (V. Pagonis).

0022-2313/$ - see front matter © 2012 Elsevier B.V. All rights reserved.
http://dx.doi.org/10.1016/j.jlumin.2012.11.046

Author's personal copy

the residual OSL signal observed after the main OSL signal has been readout. OSL signals were measured from Al_2O_3:C using blue and green light stimulation, while optical bleaching of the OSL signals was carried out using yellow, green and blue light.

Pagonis et al. [32] performed TR-OSL measurements in irradiated Al_2O_3:C powder samples using blue LEDs ($\sim$470 nm, peak power $\sim$16 mW/cm^2) and detection in the range 270–380 nm at room temperature. The two exponential fittings of the signal obtained during the relaxation period (when the optical stimulation has been turned off), gave the lifetime for the 'fast' component of 33.0 ± 0.2 ms, and for the 'slow' component in range 320 and 928 ms. These values compared well with the results obtained by Markey et al. [33] and Akselrod and McKeever [34]. This slower component in the TR-OSL relaxation signal is assumed to be due to trapping and delayed release of charges in two shallow traps (STs) during optical stimulation, and has previously been termed a delayed-OSL (DOSL) emission (see, e.g. Bøtter-Jensen et al. [1], p. 59 and references therein). Yukihara and McKeever ([35,36]) investigated the possibility of using the relative intensity of OSL emissions from F and F^+ centers as an indication of the ionization density created by the radiation, which is of interest for space, neutron, and proton dosimetry. Denis et al. ([37,38]) used continuous-wave OSL (CW-OSL) and TR-OSL measurements under pulsed laser stimulation, to investigate the components of the OSL signal from the new material Al_2O_3:C,Mg. These authors also carried out numerical simulations using a simplified kinetic model of Al_2O_3:C,Mg and described the relaxation signal using a single exponential decay plus a constant background, and obtained an F-center luminescence lifetime of $\sim$35 ms in agreement with the TR-PL measurements of Akselrod et al. [14]. Their constant background signal was attributed to phototransferred phosphorescence, caused by the presence of shallow traps above room temperature. In other notable recent work, Mishra et al. [39] and Soni et al. [40] studied deep energy levels in α-Al_2O_3:C powder using a method termed thermally assisted optically stimulated luminescence (TA-OSL). The method involves simultaneous stimulation with continuous wave optically stimulated luminescence (CW-OSL) and linear heating of the sample up to 400 °C. These authors also presented analytical expressions for the temperature dependence of optical cross-section and thermal activation energy associated with these deep traps.

The goals of this paper are as follows:

(a) To present new experimental results for TR-OSL experiments on Al_2O_3:C for stimulation temperatures between 20 and 240 °C, in which the optical stimulations are carried out using blue LEDs (470 nm).
(b) To report a new thermally assisted OSL (TA-OSL) effect, which affects the intensity of the TR-OSL signal during the optical excitation period of the measurement.
(c) To obtain the luminescence lifetime by using analytical expressions to analyze the shape of the TR-OSL signal during both the excitation and relaxation periods of the experiment. Previous published estimates of the luminescence lifetimes were obtained only by analyzing the relaxations period of TR-PL experiments.
(d) To compare the thermal quenching parameters and luminescence behavior observed using blue LEDs with those obtained in TR-PL experiments [14].
(e) To discuss the experimental results of the TR-OSL experiments in this paper within the framework of a recently proposed energy scheme (Pagonis et al. [41]).

2. Experimental

In the experimental work presented here, a single Al_2O_3:C disk supplied by Landauer Inc. is used, 5 mm in diameter by 0.9 mm thickness. Sample measurements were carried out on a Risø TL/OSL-20 reader using the same disk for all measurements (for details of the pulsed measurements see for example Ankjærgaard and Jain [42]). Blue light stimulation was performed with an LED array emitting at (470 ± 30) nm, and delivering $\sim$50 mW cm^{-2} CW-stimulation at the sample position; a 7.5 mm thick Hoya U340 filter was used to discriminate between the OSL emission and the stimulating light. Irradiations were carried out using the 40 mCi ^{90}Sr/^{90}Y β-source built into the Risø reader. The duration of the on-pulse width was set to 0.5 s and the off-time duration to 2.5 s in the results presented here.

3. Experimental results

3.1. TL measurements

The TL signal from the Al_2O_3:C disk was measured and consisted of a typical glow curve for this material, with the main dosimetric peak at $\sim$210 °C and a smaller TL peak at $\sim$70 °C corresponding to shallow traps, as shown in Fig. 1a. The disk was given a beta dose of 2 Gy, and subsequently heated at a linear heating rate of 1 °C/s and with data recorded every 1 s.

The shallow traps at $\sim$70 °C are known to influence both the luminescence intensity and apparent luminescence lifetime in this material for stimulation temperatures between room temperature and $\sim$100 °C ([14,41]).

3.2. Varying the stimulation temperature after a preheat at 240 °C

The variation of the TR-OSL signal with the stimulation temperature was studied as follows. The Al_2O_3:C disk was given a beta dose of 1 Gy and was subsequently preheated at 240 °C for 1 s, in order to nearly (but not completely) empty the dosimetric trap. This preheat treatment is administered in order to avoid any complications due to the presence of the shallow traps, known to exist in this material. In order to test whether the preheat treatment significantly alters the results of the experiments, we repeated all measurements with the same disk but without a preheat treatment, and found no significant changes occurring in the results of the experiments. The sample is next stimulated optically using blue LEDs at a variable stimulation temperatures between 20 °C and 240 °C, in steps of 10 °C. A single TR-OSL pulse was recorded for the 0.5 s duration of the optical stimulation period, and the TR-OSL signal was recorded for an additional relaxation time period of 2.5 s after the end of the single pulse. These two time periods will be referred to in the rest of this paper as the "optical stimulation period" and the "relaxation period", correspondingly.

Subsequently the sample was optically bleached for 200 s with blue light at 200 °C, in order to deplete the dosimetric trap. This experimental cycle was repeated using the same disk and for a new stimulation temperature between 20 °C and 240 °C, increasing in steps of 10 °C. Recycling measurements were performed for stimulation temperatures of 20, 100, 200 and 240 °C in order to test for sensitivity changes occurring during the experimental protocol. Very small changes in the sensitivity of the sample were observed in all experiments reported in this paper, of the order of $\sim$5% or less.

Fig. 1b shows a typical TR-OSL signal measured at room temperature, with the inset showing the same data on a semilog scale. During the optical stimulation interval 0–0.5 s the TR-OSL signal initially increases, followed by a gradual decrease. This non-monotonic pulse shape has been reported previously by Akselrod and McKeever [34], who used the pulsed optically stimulated luminescence (POSL) technique with a Nd:YAG laser

Author's personal copy

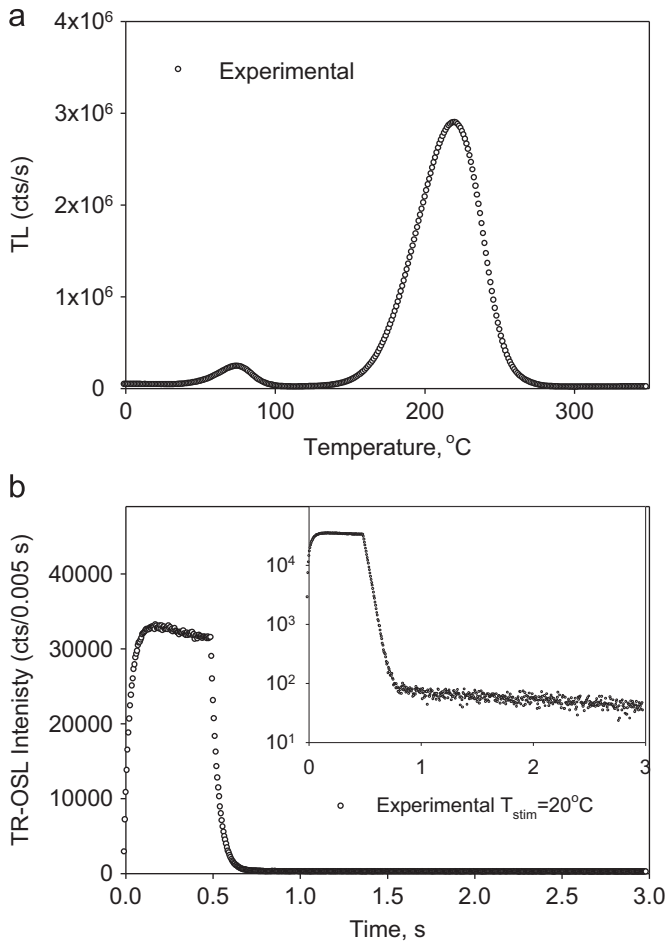

Fig. 1. (a) The TL glow curve of the Al_2O_3:C disk contains the main dosimetric peak at ~210 °C and a smaller TL peak at ~70 °C corresponding to shallow traps. The disk was given a dose of 2 Gy, and was heated at a linear heating rate of 1 °C/s. (b) Typical TR-OSL signal measured at room temperature, with the inset showing the same data on a semilog scale. During the optical stimulation interval (t=0–0.5 s) the TR-OSL signal initially increases, followed by a gradual decrease. During the relaxation period (t=0.5–3 s), the shape decays rather quickly within 0.2 s, and the inset shows the presence of a second slower component with a much longer lifetime.

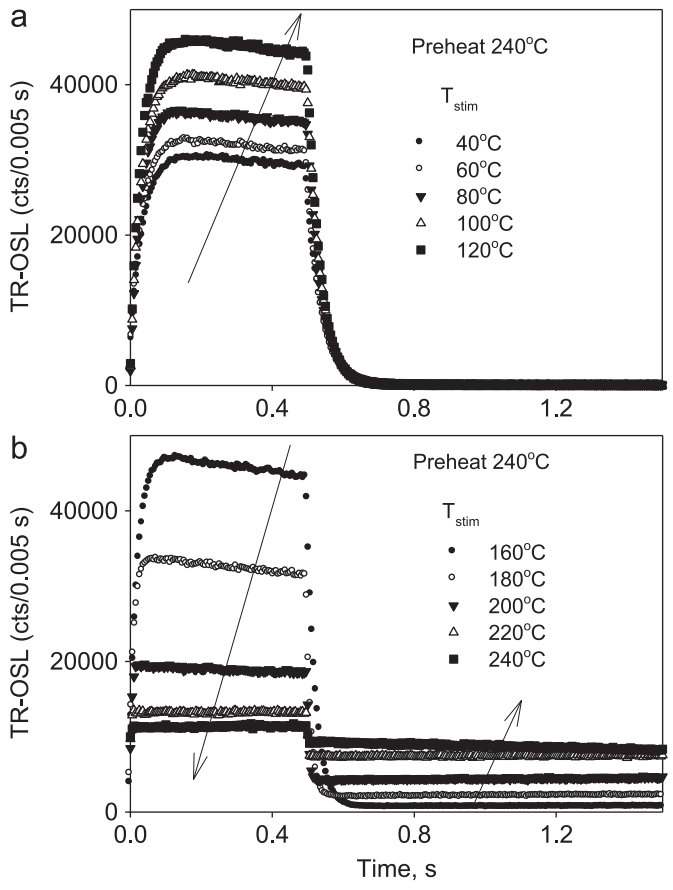

Fig. 2. (a) Typical TR-OSL signals measured at different stimulation temperatures in the range T_{stim}=40–120 °C. During optical stimulation the area under TR-OSL signal *increases* continuously, as T_{stim} increases in the direction of the arrow. The corresponding integrated TR-OSL signal during the relaxation period stays about the same at all stimulation temperatures T_{stim}, (b) TR-OSL signals measured at different stimulation temperatures in the higher temperature range T_{stim}=160–240 °C. In this temperature range, the area during the optical stimulation period *decreases* continuously as T_{stim} increases in the direction of the arrow. The corresponding integrated TR-OSL signal during the relaxation period *increases* as T_{stim} increases.

operated at a laser pulse frequency of 4000 Hz. In this technique, data acquisition occurs only for a predefined period between each pulse, by synchronizing the stream of laser pulses with a PMT gate. These authors explained the non-monotonic shape of the pulses as follows. The intensity of the signal initially increases until equilibrium is established between the rate of excitation of luminescence centers and the rate of decay of these centers due to the high power of the laser. After equilibrium is established, the signal decreases due to the emptying of the dosimetric trap. Several examples of these non-monotonic pulses are shown in their Fig. 5 of Ref. [34], and an additional example is given in Ref. [1], p. 328, Fig. 7.9. This type of non-monotonic pulse shape has also been reported previously for a variety of luminescence materials like quartz, and NaCl [32].

Fig. 2a shows the TR-OSL signal measured at 5 different stimulation temperatures (T_{stim}) in the range T_{stim}=40–120 °C, while Fig. 2b demonstrates typical results in the higher temperature range T_{stim}=160–240 °C. These data demonstrate the existence of two very different behaviors of the TR-OSL signal at these two stimulation temperature ranges. For low stimulation temperatures T_{stim} < 120 °C shown in Fig. 2a, the intensity of the TR-OSL signal during the optical excitation period *increases* continuously as T_{stim} increases, in the direction of the arrow in the figure. However, Fig. 2b shows that for T_{stim} > 150 °C, the TR-OSL intensity during the optical excitation period *decreases* continuously as T_{stim} increases, in the direction of the arrow in the figure. Furthermore, Fig. 2a shows that the intensity of the TR-OSL signal during the *relaxation* period stays almost constant at all stimulation temperatures T_{stim}, while in Fig. 2b this signal intensity *increases* as T_{stim} increases, again in the direction of the arrow.

These changes with the stimulation temperature are shown more clearly in Fig. 3a which shows the *integrated* TR-OSL signal during the optical stimulation (curve **1**, open circles) and during the relaxation periods (curve **2**, solid circles), as a function of the stimulation temperature. The data in both curves **1** and **2** have been divided by the corresponding lengths of the optical stimulation and relaxation periods (0.5 s and 2.5 s correspondingly), in order to account for the fact that these two periods are unequal. The data in curve **1** of Fig. 3a indicates the presence of a thermally assisted OSL (TA-OSL) process, which causes the integrated TR-OSL signal to increase between 50 and 150 °C. This TA-OSL effect has not been previously reported for TR-OSL experiments in alumina, but has been well documented in the case of quartz samples (Ref. [1], page 179, their Fig. 5.48; see also the extensive list of references and activation energy values in Ref. [7]). The slight decrease of the luminescence intensity seen in curve 1 for stimulation temperatures below 50 °C has been shown previously

Author's personal copy

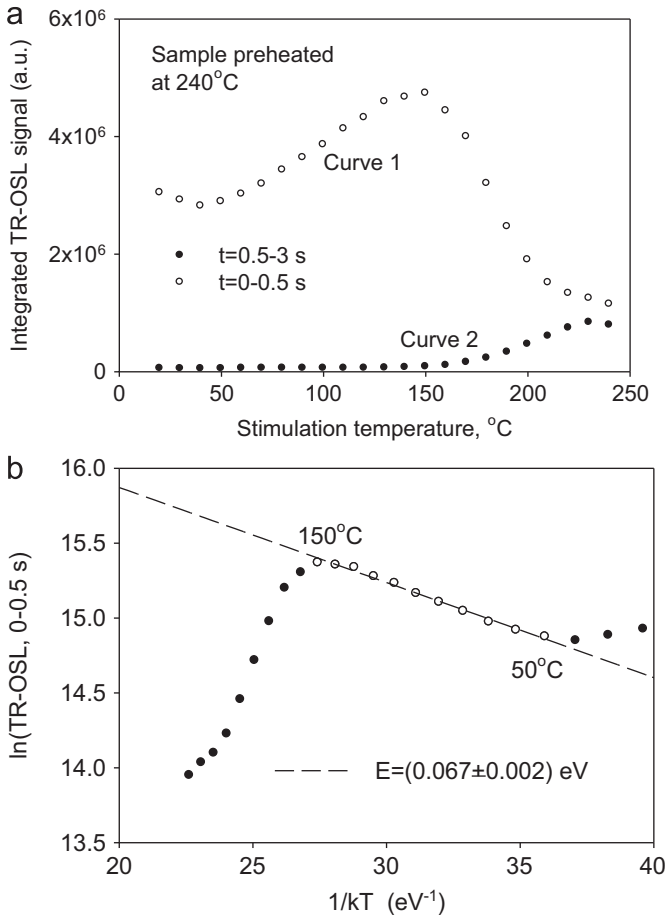

Fig. 3. (a) The integrated TR-OSL signal from Fig. 2 is shown as a function of the stimulation temperature, during the optical stimulation period (curve **1**, open circles). The initial increase in curve **1** between 50 and 120 °C indicates the presence of a thermally assisted luminescence process. At higher temperatures the integrated TR-OSL signal in curve **1** decreases, due to thermal quenching effects. The corresponding integrated TR-OSL signal during the relaxation periods (curve **2**, solid circles) shows the presence of a thermally activated process at higher stimulation temperatures. (b) Arrhenius analysis of the integrated TR-OSL signal from curve **1** in (a). The straight line fit between stimulation temperatures of 50 °C and 150 °C yields the activation energy for the thermally assisted OSL (TA-OSL) process $E_{th}=0.067\pm0.002$ eV.

by experiment and modeling to be caused by the influence of the shallow traps corresponding to the TL peak at ~70 °C shown in Fig. 1a ([14,41]).

At higher stimulation temperatures the integrated TR-OSL signal in curve **1** decreases, due to the dominance of thermal quenching effects. Fig. 3b shows an Arrhenius analysis for the integrated TR-OSL signal during the optical stimulation period. From the straight line fit of the data between stimulation temperatures of 50 °C and 150 °C in Fig. 3b, an estimate of the activation energy for the TA-OSL process is obtained $E_{th}=0.067\pm0.002$ eV. This represents the activation energy for the TA-OSL process in alumina during the short blue light pulses used in this experiment. It is noted that the type of TA-OSL phenomenon reported in Fig. 3a may or may not be related to a TA-OSL effect reported by Mishra et al. [39] and Soni et al. [40]. These authors used a very different technique than the TR-OSL measurements in this paper, by combining continuous-wave OSL stimulation (CW-OSL) of the sample, simultaneously with linear heating with a constant heating rate up to 400 °C. Well-defined TA-OSL peaks were correlated to two different types of deeper defects, and the activation energies of the TA-OSL signals were found to be 0.268 eV and 0.485 eV. Further experimental and modeling work is necessary to ascertain whether their type of experiment measures the same TA-OSL phenomenon as the TR-OSL experiments reported in this paper.

The signal shown as curve 2 in Fig. 3a is a thermally activated component which is also present during the corresponding optical stimulation period. As discussed in the introduction, this part of the signal represents a phosphorescence component previously reported as a "delayed OSL" phenomenon in this material [1,2]. The *net* integrated TR-OSL intensity is therefore obtained by subtracting curves 1 and 2 in Fig. 3a, and is shown in Fig. 4 as a function of the stimulation temperature (open triangles). This net TR-OSL intensity initially increases at low stimulation temperatures, before it decreases according to thermal quenching at higher temperatures. The data in Fig. 4 can be fitted to the following empirical equation, which can be used to evaluate the three parameters C', W and E_{th} [41]:

$$I(T)=\frac{I_o\exp(-E_{th}/k_BT)}{1+C'\exp(-W/k_BT)} \quad (1)$$

where the constant C' is a dimensionless quantity, W represents the activation energy of the thermal quenching process, k_B is the Boltzmann constant, T is the temperature of the sample, I_o is the luminescence intensity at low temperatures. The parameter E_{th} represents the activation energy of the thermally assisted luminescence process in the material.

The results of a least squares fit to the experimental data are shown as a solid line in Fig. 4. The values of the least squares fitting parameters obtained from the solid line in Fig. 4 are $W=(1.032\pm0.005)$ eV, $C'=(2.9\pm1.7)\times10^{11}$ and $E_{th}=(0.072\pm0.008)$ eV. This value of thermal activation energy E_{th} is in close agreement with the value obtained from the Arrhenius plot in Fig. 3b, namely $E_{th}=0.067\pm0.002$ eV. It is noted that this type of analysis has also been carried out previously for quartz and feldspar samples (see for example Ref. [1], pages 179 and 193, Fig. 5.48). The thermal quenching parameters obtained using this method are also similar to the average published values of $W=(1.08\pm0.03)$ eV and $C'=(3.6\pm2.9)\times10^{12}$ measured in the TR-PL experiments of Akselrod et al. [14]. The disagreement between Eq. (1) and the experimental data at low temperatures in Fig. 4 is due to the well-known effects of shallow traps in this material ([14,41]).

It is noted that the activation energy of thermal assistance $E_{th}=(0.072\pm0.008)$ eV has a meaning and affects the results of the experiment only at low temperatures. As shown in Fig. 3a (curve 1) and in Fig. 3b, the integrated luminescence intensity increases for a low temperature range between 50 °C and 150 °C.

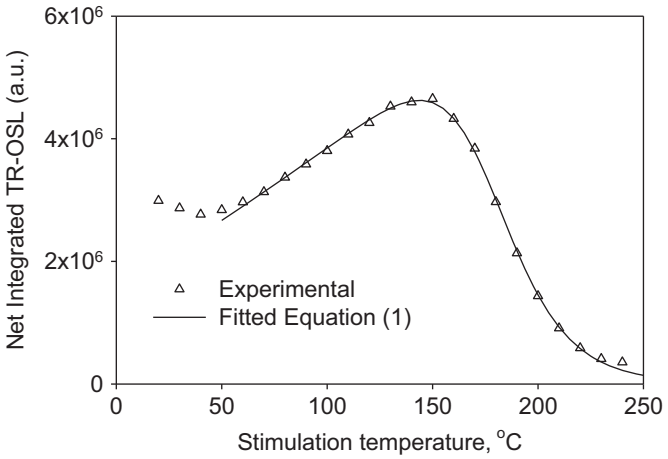

Fig. 4. The net integrated TR-OSL intensity from Fig. 3a, is shown as a function of the stimulation temperature and is fitted to the empirical Eq. (1).

Author's personal copy

For temperatures above 150 °C, this thermally assisted effect and the associated energy lose their meaning, since they are overtaken by the much larger effects of thermal quenching and by the activation energy of the main TL dosimetric trap. This is shown in Fig. 3a, where the integrated intensity starts to decrease after 150 °C.

3.3. The luminescence lifetimes

By mathematically analyzing the shapes of the TR-OSL pulses measured at different stimulation temperatures, it is possible to estimate the luminescence lifetimes associated with the optical excitation period and the relaxation periods. Yukihara and McKeever [2] derived analytical expressions for the TR-OSL intensity by writing the rate equations for the time dependent concentration of excited luminescence centers $m^*(t)$, and for the concentration $n(t)$ of trapped electrons in the dosimetric trap during the optical stimulation period. Their expression for the luminescence intensity $I_{ON}(t)$ during the optical stimulation period is (Ref. [2], Eq. 2.41, p. 52):

$$I_{ON}(t) \propto m_0^* e^{-t/\tau} + \frac{n_0 p}{-p+1/\tau}\left(e^{-pt} - e^{-t/\tau}\right) \tag{2}$$

where m_0^*, n_0 represent the initial concentrations at the beginning of each stimulation pulse (time $t=0$), τ is the luminescence lifetime and p is the probability of photoionization of the trapping centers. These authors also wrote an analytical expression for the luminescence intensity $I_{OFF}(t)$ as a function of time after the optical stimulation has been turned off, as follows ([2], p. 52, Eq. 2.43):

$$I_{OFF}(t) \propto m^*(\Delta t) e^{-t/\tau} \tag{3}$$

where $m^*(\Delta t)$ represents the concentration of excited centers at the end of the stimulation period of duration Δt. In principle one assumes that the luminescence lifetimes in Eqs. (2) and (3) will be the same. Therefore, the experimental data in Fig. 2 are fitted empirically using the same values of the luminescence lifetimes τ during both the optical excitation period ($t=0$–0.5 s), and during the relaxation period (0.5–3 s). Also the inset data in Fig. 1b shows clearly that the TR-OSL intensity contains a slow luminescence component with a much longer luminescence lifetime; this slower thermal component will be present during both the optical excitation and the relaxation periods. Therefore the TR-OSL pulses in Fig. 2a and b are fitted to the following two expressions:

$$I_{ON}(t) = Ae^{-t/\tau} + \frac{Bp}{-p+1/\tau}\left(e^{-pt} - e^{-t/\tau}\right) + De^{-t/\tau_{SLOW}}, \quad t < t_o \tag{4}$$

$$I_{OFF}(t) = Ce^{-t/\tau} + De^{-t/\tau_{SLOW}} \quad t > t_o, \tag{5}$$

where t_o is the duration of the optical stimulation ($t_o=0.5$ s per scan in these experiments), A, B, C, D are fitting constants, τ_{SLOW} is the luminescence lifetime of the slow component during the relaxation period, and τ represents the luminescence lifetime. The common exponential term $De^{-t/\tau_{SLOW}}$ in Eqs. (4) and (5) represents the optically stimulated phosphorescence signal previously reported as a "delayed OSL" phenomenon in this material [1,2,14].

Fig. 5a and b shows typical results from analysis of the TR-OSL signals using Eqs. (4) and (5), at two relatively low stimulation temperatures of 20 and 100 °C. The residuals of the fitting procedure are shown below the fitted graphs, and are seen to be better than ~1–2% of the corresponding TR-OSL intensity, and for all points along the TR-OSL pulse. Typical R^2 values for these fits are $R^2=0.9998$, indicating very good fits to the data. Fig. 6a and b shows typical results from analysis of the TR-OSL signals using Eqs. (4) and (5), at two relatively high stimulation temperatures of 170 and 220 °C. The residuals for these higher stimulation temperatures are also smaller than 1–2 %.

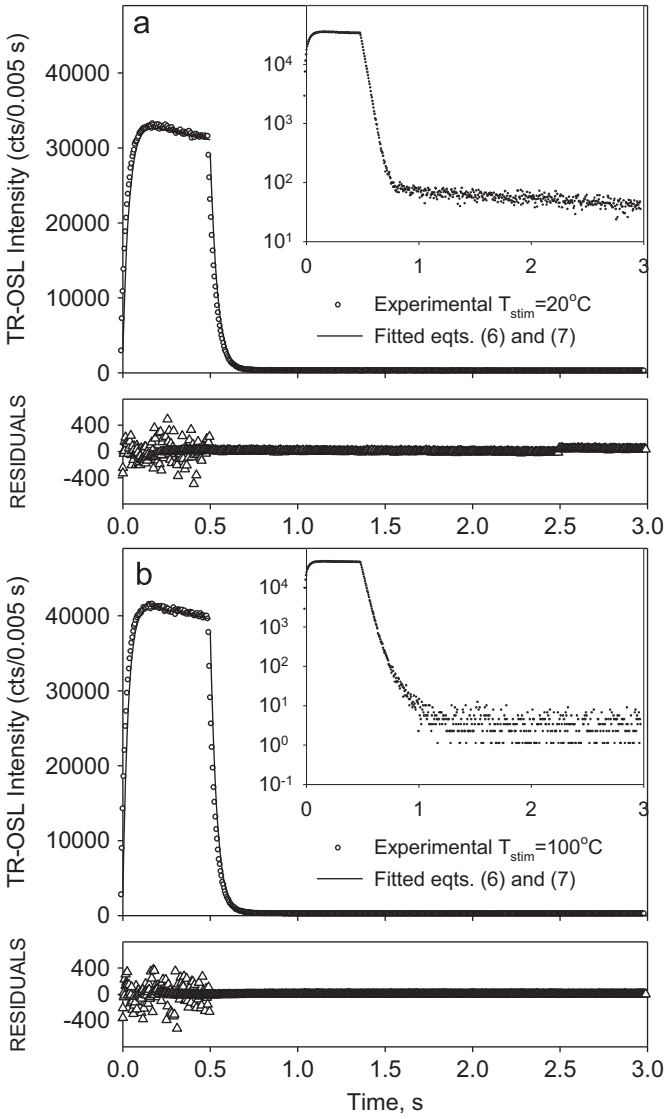

Fig. 5. Typical results for the analysis of the TR-OSL signals at two low stimulation temperatures of (a) 20 °C and (b) 100 °C. The residuals of the fitting procedure are shown below the fitted graphs, and are smaller than 2% of the corresponding TR-OSL intensity, at all points along the TR-OSL pulse. Typical R^2 values for these fits are $R^2=0.9998$ indicating very good fits to the data.

Fig. 7 shows the luminescence lifetimes τ obtained from analyzing the data in Fig. 2, as a function of the stimulation temperature. The τ values decrease from a value of ~37 ms at room temperature to a value of ~2 ms at 210 °C. The higher values of τ shown at low stimulation temperatures $T_{stim} < 60$ °C in Fig. 7 are due to the well-known influence of the shallow traps in this material ([14, 2,3, 41]). For stimulation temperatures above 210 °C scattering in the experimental data does not allow correct determination of lifetimes smaller than ~2 ms.

The luminescence lifetime τ will have contributions from radiative processes, from non-radiative transitions, and from phonon-assisted processes present in the material (Akselrod et al. [14], Pagonis et al. [41]). The temperature-dependent lifetime $\tau(T)$ depends on the stimulation temperature T according to (Akselrod et al. [14], their Eq. 2):

$$\tau(T) = \frac{\tau_{rad}}{1 + C' \exp(-W/k_B T)}, \tag{6}$$

Author's personal copy

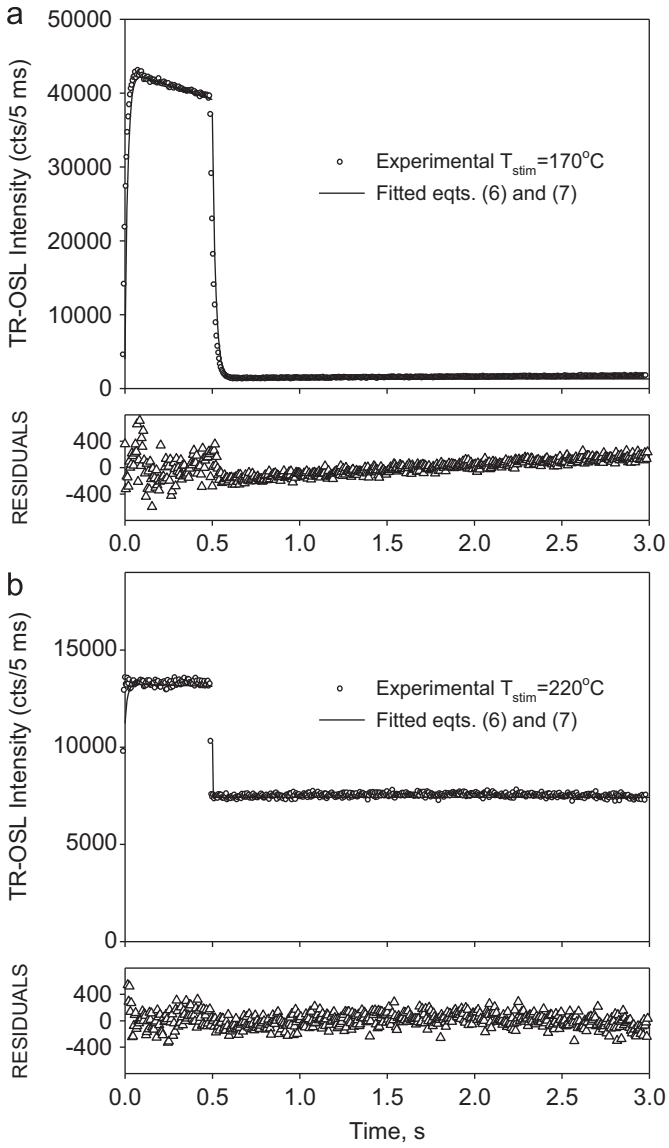

Fig. 6. Two examples of fitting the TR-OSL pulses at higher stimulation temperatures of (a) 170 °CC and (b) 220 °C. Analysis of the data shows that the presence of a thermally activated background component, which is strongly dependent on the stimulation temperature for $T_{stim} > 160$ °C. This component has been previously reported as "delayed OSL" in this material.

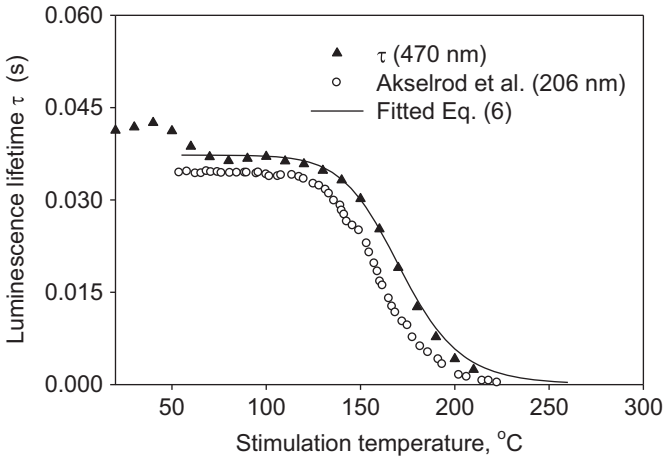

Fig. 7. The luminescence lifetimes τ obtained from analyzing the data in Fig. 2 using Eqs. (4) and (5), as a function of the stimulation temperature. The accuracy of these luminescence lifetimes is estimated at ± 1 ms or better. The luminescence lifetimes τ from the TR-PL experiments of Akselrod et al. [14] using UV pulses (~205 nm) are also shown for comparison purposes.

where τ_{rad} is the lifetime for the radiative recombination process at room temperature, and C' and Wrepresent the same thermal quenching parameters as in Eq. (1). The phonon contribution to τ is ignored in this equation. As the temperature T of the sample is increased during the measurement, we expect the lifetime $\tau(T)$ of the charge carriers in the sample to decrease according to Eq. (6).

The data in Fig. 7 can be fitted to the empirical Eq. (6), in order to evaluate the thermal quenching parametersC', W. The results of a least squares fit to the experimental data are shown as a solid line in Fig. 7. Once more, the disagreement between Eq. (6) and the experimental data at low temperatures in Fig. 7 is attributed to the well-known effects of shallow traps in this material [14]. The values of the least squares fitting parameters obtained from the solid best fit line in Fig. 7, are $W=1.075$ eV, $C'=1.3\times10^{12}$. These values of C', W are in reasonable agreement with the values obtained using Eq. (1), and with the broad average values of $W=(1.08\pm0.03)$ eV and $C'=(3.6\pm2.9)\times10^{12}$ reported by Akselrod et al. [14].

It is estimated that the accuracy of obtaining the values of τ using Eqs. (4) and (5) is ± 1 ms or better. These results are also similar to previous experimental and modeling work for *quartz*, which showed that the same values of the luminescence lifetimes are obtained from either one of the two periods in the TR-OSL signal ([32] and references therein). The new experimental data shown in Fig. 7 are then consistent with the assumption that the apparent luminescence lifetimes in a TR-OSL experiment are affected only by the stimulation temperature and by thermal quenching, as indicated for example by the empirical Eq. (6). The luminescence lifetimes τ in Fig. 7 seem to be systematically higher than the average values reported from TR-PL experiments using UV pulses [2], which are shown as open circles in Fig. 7. Further experimental and modeling work is necessary in order to verify or refute whether these differences in luminescence lifetimes observed during TR-OSL and TR-PL experiments are due to sample variations, or due to some other effect present in these TR-OSL experiments.

The other important experimental parameter that can be extracted from analyzing the shape of the pulses using Eqs. (4) and (5), is the probability p of photoionization of the trapping centers. This probability p was found to be constant at all stimulation temperatures within experimental error, with an average value of $p=(0.20\pm0.05)$ s^{-1}.

3.4. Discussion of luminescence mechanism during TR-OSL and TR-PL experiments

In this section, the experimental results are discussed within the framework of a kinetic model which has been proposed for this material. The purpose of this discussion is to point out some major differences between the physical processes taking place during TR-OSL and TR-PL experiments. The relevant model is shown schematically in Fig. 8a for TR-PL experiments, and as a modified version in Fig. 8b for TR-OSL experiments.

Nikiforov et al. [45] developed the original kinetic model which provides a description of the effect of thermal quenching on several luminescence phenomena in Al_2O_3:C. Pagonis et al. [41] used a modified version of this model to simulate time-resolved photoluminescence (TR-PL) experiments in α-Al_2O_3:C. The effect of shallow traps on the luminescence lifetimes was also studied and compared with available experimental data. The modified energy diagram arrived at by Pagonis et al. [41] and

Author's personal copy

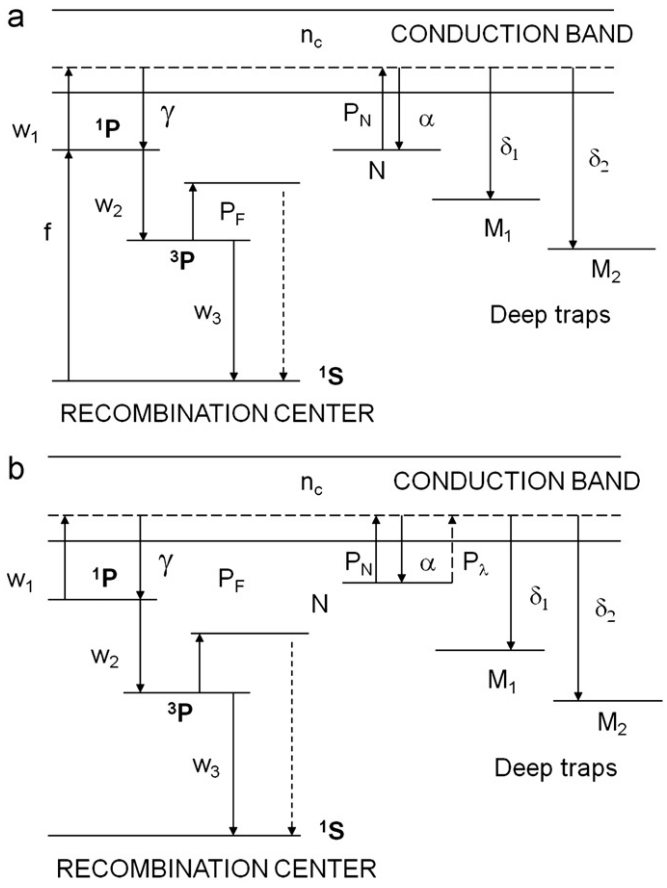

Fig. 8. (a) The energy scheme and kinetic model of Nikiforov et al. [45], as modifed by Pagonis et al. [41]. Transitions shown are typical for a TR-PL experiment which uses short UV-pulses. (b) The same energy scheme as in (a), with transitions shown for a TR-OSL experiment which uses short 470 nm LED pulses. The additional transition P_λ shown as a dashed line occurs during excitation with blue light, and can be described mathematically by the expression $P_\lambda = \lambda \exp(-E_{th}/kT)$, as discussed in the text.

the relevant transitions are shown in Fig. 8a. The key element of this model is the very high probability of photoionization of F-centers during TR-PL experiments. The electron structure of F-centers in aluminum oxide is considered to be similar to the structure of a helium quasi-atom (Evans [44]). The ground state of the recombination center in Fig. 8a is characterized by the 1S level, while the excited states are considered to be a singlet (1P) and a triplet (3P) state. Excitation of an F-center corresponds to the 1 S→ 1 P transition. Excitation by UV light at ~205 nm leads to optical ionization of F-centers and the subsequent capture of electrons through the conduction band (CB) into electron traps. Other symbols shown in Fig. 8a and b are: N denotes the main dosimetric trap, M_1 and M_2 stand for deep electron traps. Upon optical excitation in the absorption band, the center is excited to the 1P state via the transition indicated by f in Fig. 8a, and luminescence of an F-center (centered at ~420 nm) corresponds to the transition w_3. Thermal ionization of the excited 3P state corresponds to the transition indicated as P_F, given by the Boltzmann factor $P_F = C\exp(-W/kT)$, where W is the activation energy of the thermal quenching process and C is a dimensionless constant. Thermal ionization leads to a decrease in the fraction of radiative transitions (w_3) taking place at the center, and is believed to be the direct cause of thermal quenching of luminescence in this material. The optical transition denoted by w_1 results in the formation of an F^+-center and free electrons which result from the ionization of F-centers, can be captured in dosimetric or deep traps. The probability of thermal emptying for the dosimetric traps is indicated as transition P_N in Fig. 8a and b, and is described mathematically by the expression $P_N = s\exp(-E/kT)$, here E is the trap depth of the main dosimetric trap and s is the corresponding frequency factor. For a detailed simulation of the effect of thermal quenching on the TL glow curves of dosimetric materials the reader is referred to the work by Subedi et al. [43].

Photons of UV light (~205 nm) used during TR-PL experiments have enough energy to photoionize the F-centers in the material. On the contrary, one does not expect blue light photons with a wavelength of 470 nm used in TR-OSL experiments to have enough energy to cause photoionization. One might therefore expect that during TR-OSL experiments, the dominant process would be blue light photons exciting electrons directly out of the main dosimetric trap, while the probability of photoionization of F-centers will be negligible. Transition f is then missing from Fig. 8b. The additional transition P_λ occurring during excitation with blue light is shown as a dashed line in Fig. 8b, and can be described mathematically by the expression $P_\lambda = \lambda \exp(-E_{th}/kT)$, where λ is the probability of optical excitation and E_{th} represents the thermal activation energy of the TA-OSL process discussed previously.

According to this proposed scheme shown in Fig. 8b, during the TR-OSL experiment electrons are raised from the dosimetric trap into the conduction band, they get trapped subsequently into the various traps and centers, and eventually participate in the complex luminescence process known to take place within the F-centers. TA-OSL effects described by the transition P_λ are present during the optical stimulation and become important between temperatures between 50 and 150 °C, but are absent during the relaxation periods. Further experimental work using light of different wavelengths as well as different experimental conditions like irradiation dose, preheat, and different samples would be very useful in further elucidating the luminescence mechanism.

4. Conclusions

This paper presented new TR-OSL experiments for Al_2O_3:C using blue LEDs (470 nm). The luminescence lifetimes were estimated as a function of stimulation temperature by using analytical expressions to analyze the non-monotonic shape of the TR-OSL signal during both the excitation and relaxation periods of the experiment. Previous estimates of the luminescence lifetimes were obtained only by analyzing the relaxations period of TR-PL experiments. The results show that both periods of the TR-OSL experiment can be described by the same luminescence lifetime. The values of the thermal quenching parameters C', W obtained using blue LEDs are consistent with those obtained in TR-PL experiments (Akselrod et al. [14]).

The integrated intensity of the TR-OSL signal was also analyzed using analytical expressions, and a new TA-OSL effect is reported for excitation with blue LEDs for stimulation temperatures between 50 and 150 °C, with a thermal activation energy $E_{\rm th} = (0.067 \pm 0.002)$ eV. The thermal quenching parameters C', W obtained from analyzing the intensity as a function of stimulation temperature are consistent with those obtained from the temperature dependence of the luminescence lifetimes.

References

[1] L. Bøtter-Jensen, S.W.S. McKeever, A.G. Wintle, Optically Stimulated Luminescence Dosimetry, Elsevier, Amsterdam, 2003.
[2] E.G. Yukihara, S.W.S. McKeever, Optically Stimulated Luminescence: Fundamentals and Applications, Wiley, New York, 2011.
[3] R. Chen, V. Pagonis, Thermally and Optically Stimulated Luminescence: A Simulation Approach, Wiley, Chichester, 2011.
[4] I.K Bailiff, Radiat. Meas. 32 (2000) 401.

Author's personal copy

[5] M.L. Chithambo, R.B. Galloway, Meas. Sci. Technol. 11 (2000) 418.
[6] M.L. Chithambo, F. Preusser, K. Ramseyer, F.O. Ogundare, Radiat. Meas. 42 (2007) 205.
[7] M.L. Chithambo, Radiat. Meas. 37 (2003) 167.
[8] D.C.W. Sanderson, R.J. Clark, Radiat. Meas. 23 (1994) 633.
[9] R.J. Clark, I.K. Bailiff, Radiat. Meas. 29 (1998) 553.
[10] S. Tsukamoto, P.M. Denby, A.S. Murray, L. Bøtter-Jensen, Radiat. Meas. 41 (2006) 790.
[11] P.M. Denby, L. Bøtter-Jensen, A.S. Murray, K.J. Thomsen, P. Moska, Radiat. Meas. 41 (2006) 774.
[12] P. Morthekai, J. Thomas, M.S. Padian, V. Balaram, A.K. Singhvi, Radiat. Meas. 47 (2012) 857.
[13] M. Jain, C. Ankjærgaard, Radiat. Meas. 46 (2011) 292.
[14] M.S. Akselrod, N. Agersnap Larsen, V. Whitley, S.W.S. McKeever, J. Appl. Phys. 84 (1998) 3364.
[15] M.S. Akselrod, N. Agersnap Larsen, V. Whitley, S.W.S. McKeever, Radiat. Prot. Dosim. 84 (1999) 39.
[16] I.I. Milman, V.S. Kortov, S.V. Nikiforov, Radiat. Meas. 29 (1998) 401.
[17] G. Kitis, Phys. Stat. Sol. A, Appl. Res. 191 (2002) 621.
[18] E.G. Yukihara, V.H. Whitley, J.C. Polf, D.M. Klein, S.W.S. McKeever, A.E. Akselrod, M.S. Akselrod, Radiat. Meas. 37 (2003) 627.
[19] V.H. Whitley, S.W.S. McKeever, J. Appl. Phys. 87 (2000) 249.
[20] J.C. Polf, E.G. Yukihara, M.S. Akselrod, S.W.S. McKeever, Radiat. Meas. 38 (2004) 227.
[21] L.E. Colyott, M.S. Akselrod, S.W.S. McKeever, Radiat. Prot. Dosim. 65 (1996) 263.
[22] N. Agersnap Larsen, Ph.D. Thesis, Risø National Laboratory, Roskilde, Denmark. Available from: 〈http://www.risoe.dk/rispubl/NUK/ris-r-1090.htm〉, 1999.
[23] N. Agersnap Larsen, L. Bøtter-Jensen, S.W.S. McKeever, Radiat. Prot. Dosim. 84 (1999) 87.
[24] V.S. Kortov, I.I. Milman, S.V. Nikiforov, Radiat. Prot. Dosim. 84 (1999) 35.
[25] V.S. Kortov, I.I. Milman, S.V. Nikiforov, E.V. Moiseĭkin, Phys. Solid State 48 (2006) 447.
[26] J.M. Edmund, C.E. Andersen, Radiat. Meas. 42 (2007) 177.
[27] E. Bulur, H.Y. Göksu, Radiat. Meas. 30 (1999) 203.
[28] D. Emfietzoglou, M. Moscovitch, Radiat. Prot. Dosim. 65 (1996) 259.
[29] L. Oster, D. Weiss, N. Kristianpoller, J. Phys. D: Appl. Phys. 27 (1994) 1732.
[30] G.S. Polymeris, S. Raptis, D. Afouxenidis, N.C. Tsirliganis, G. Kitis, Radiat. Meas. 45 (2010) 519.
[31] N.K. Umisedo, E.M. Yoshimura, P.B.R. Gasparian, E.G. Yukihara, Radiat. Meas. 45 (2010) 151.
[32] V. Pagonis, S.M. Mian, M.L. Chithambo, E. Christensen, C.J. Barnold, Phys. D: Appl. Phys. 42 (2009) 055407.
[33] B.G. Markey, S.W.S. McKeever, M.S. Akselrod, L. Bøtter-Jensen, N. Agersnap Larsen, L.E. Colyott, Radiat. Prot. Dosim. 65 (1996) 185.
[34] M.S. Akselrod, S.W.S. McKeever, Radiat. Prot. Dosim. 81 (1999) 167.
[35] E.G. Yukihara, S.W.S. McKeever, J. Appl. Phys. 100 (2006) 083512.
[36] E.G. Yukihara, S.W.S. McKeever, Radiat. Prot. Dosim. 119 (2006) 206.
[37] G. Denis, M.G. Rodriguez, M.S. Akselrod, T.H. Underwood, E.G. Yukihara, Radiat. Meas. 46 (2011) 1457.
[38] G. Denis, M.S. Akselrod, E.G. Yukihara, J. Appl. Phys. 109 (2011) 104906 http://dx.doi.org/10.1063/1.3584791.
[39] D.R. Mishra, A. Soni, N.S. Rawat, M.S. Kulkarni, B.C. Bhatt, D.N. Sharma, Radiat. Meas. 46 (2011) 635.
[40] A. Soni, D.R. Mishra, B.C. Bhatt, S.K. Gupta, N.S. Rawat, M.S. Kulkarni, D.N. Sharma, Radiat. Meas. 47 (2012) 111.
[41] V. Pagonis, R. Chen, J.W. Maddrey, B. Sapp, J. Lumin. 131 (2011) 1086.
[42] C. Ankjærgaard, M. Jain, J. Phys. D: Appl. Phys. 43 (2010) 255502 12 pp.
[43] B. Subedi, G. Kitis, V. Pagonis, Phys. Status Solidi A 207 (2010) 1216.
[44] B.D. Evans, J. Nucl. Mater. 219 (1996) 202.
[45] S.V. Nikiforov, I.I. Milman, V.S. Kortov, Radiat. Meas. 33 (2001) 547.